Eur Radiol (2008) 18: 530–537
DOI 10.1007/s00330-007-0778-8

Klaus Kurt Gast
Alexander Biedermann
Annette Herweling
Wolfgang Günter Schreiber
Jörg Schmiedeskamp
Eckhard Mayer
Claus Peter Heussel
Klaus Markstaller
Hans-Ulrich Kauczor
Balthasar Eberle

Oxygen-sensitive ^{3}He-MRI in bronchiolitis obliterans after lung transplantation

Received: 12 April 2007
Revised: 31 July 2007
Accepted: 27 August 2007
Published online: 10 October 2007

K. K. Gast (✉)
Klinik und Poliklinik für diagnostische und interventionelle Radiologie, Klinikum der Johannes Gutenberg-Universität, Langenbeckstrasse 1, 55131 Mainz, Germany
e-mail: kgast@radiologie.klinik.uni-mainz.de
Tel.: +49-6131-172019
Fax: +40-6131-176633

A. Biedermann
3. Medizinische Klinik, Pulmonologie, Klinikum der Johannes Gutenberg-Universität, Langenbeckstrasse 1, 55131 Mainz, Germany

A. Herweling
Klinik für Anästhesiologie, Klinikum der Johannes Gutenberg-Universität, Langenbeckstrasse 1, 55131 Mainz, Germany

W. G. Schreiber
Klinik und Poliklinik für diagnostische und interventionelle Radiologie, MR-Physik, Klinikum der Johannes Gutenberg-Universität, Langenbeckstrasse 1, 55131 Mainz, Germany

J. Schmiedeskamp
Max-Planck-Institut für Polymerforschung, Ackermannweg 10, 55128 Mainz, Germany

E. Mayer
Klinik für Herz-, Thorax- und Gefässchirurgie, Klinikum der Johannes Gutenberg-Universität, Langenbeckstrasse 1, 55131 Mainz, Germany

C. P. Heussel
Abteilung für Radiologie, Thoraxklinik Heidelberg, Amalienstr. 5, 69126 Heidelberg, Germany

K. Markstaller · B. Eberle
Klinik für Anästhesiologie, Inselspital/Universitätsspital, 3010 Bern, Switzerland

H.-U. Kauczor
Radiologie, Deutsches Krebsforschungszentrum (DKFZ), Im Neuenheimer Feld 280, 69120 Heidelberg, Germany

Abstract Oxygen-sensitive ^{3}He-MRI was studied for the detection of differences in intrapulmonary oxygen partial pressure (pO_2) between patients with normal lung transplants and those with bronchiolitis obliterans syndrome (BOS). Using software developed in-house, oxygen-sensitive ^{3}He-MRI datasets from patients with normal lung grafts (n=8) and with BOS (n=6) were evaluated quantitatively. Datasets were acqiured on a 1.5-T system using a spoiled gradient echo pulse sequence. Underlying diseases were pulmonary emphysema (n=10 datasets) and fibrosis (n=4). BOS status was verified by pulmonary function tests. Additionally, ^{3}He-MRI was assessed blindedly for ventilation defects. Median intrapulmonary pO_2 in patients with normal lung grafts was 146 mbar compared with 108 mbar in patients with BOS. Homogeneity of pO2 distribution was greater in normal grafts (standard deviation pO2 34 versus 43 mbar). Median oxygen decrease rate during breath hold was higher in unaffected patients (−1.75 mbar/s versus −0.38 mbar/s). Normal grafts showed fewer ventilation defects (5% versus 28%, medians). Oxygen-sensitive ^{3}He-MRI appears capable of demonstrating differences of intrapulmonary pO2 between normal lung grafts and grafts affected by BOS. Oxygen-sensitive ^{3}He-MRI may add helpful regional information to other diagnostic techniques for the assessment and follow-up of lung transplant recipients.

Keywords Lung · Transplantation · Helium · MRI · Oxygen

Introduction

^{3}He-MRI is a novel technique for functional imaging of the lung. A variety of different pulse sequence types have been described, including spin density, diffusion-weighted, dynamic ventilation and oxygen-sensitive imaging [1–4]. Spin density and dynamic imaging have been applied to lung transplant recipients with the aim to improve non-invasive image-based diagnostics of obliterative bronchiolitis (OB) [5, 6]. In a follow-up study, spin density imaging detected OB earlier than pulmonary function tests in two out of five cases [7].

Pulmonary function testing (PFT) is widely used as the standard diagnostic tool for the follow-up of lung transplant recipients. Transbronchial lung biopsies can confirm clinical suspicion of bronchiolitis obliterans syndrome (BOS). Both approaches have inherent disadvantages. PFT remains a global screen in which functional impairment of lung regions affected by OB may be compensated for by healthy regions [8]. Bronchoscopy with transbronchial biopsy is invasive. Due to the inhomogeneous distribution of OB, foci of disease can be missed [9]. Computed tomography (CT), the standard imaging method in lung transplant recipients, is only moderately sensitive in the detection of OB [10].

^{3}He-MRI is a sensitive method to detect ventilatory disturbances in a variety of lung diseases [11–14]. Patients with a clinical diagnosis of BOS show an increased incidence of ventilation defects when compared with patients with a normal lung graft [7]. Since in OB ventilation becomes impaired by obliteration of small airways, impaired pulmonary gas exchange may reduce local alveolar oxygen partial pressure (pO_2) even before a lung region shows signal loss due to attenuated ^{3}He intake. Oxygen-sensitive ^{3}He-MRI has been validated as a non-invasive method to measure the regional distribution of intrapulmonary pO_2 [15, 16].

In oxygen-sensitive ^{3}He-MRI the T1-shortening effect of molecular oxygen is used to calculate the pO_2 in a respective volume of interest by signal intensity changes in repeated imaging during a single breath-hold. Intrapulmonary pO_2 is the result of a local steady-state balance between alveolar ventilation and perfusion of the pulmonary capillary bed, i.e. a regional $\dot{V}_A/Q$ ratio. Since BO is an airway disease, ventilation becomes impaired in affected regions of the lung. Perfusion will adapt to these changes depending on the responsiveness of hypoxic pulmonary vasoconstriction. In a state of local alveolar hypoventilation, the resultant decrease of intrapulmonary pO_2 is expected to be compensated for, at least partially, by adaptive changes in perfusion. Nevertheless, the distribution of $\dot{V}_A/Q$ ratios and hence, intrapulmonary pO_2 values, would be expected to widen. Even more so, since BO itself is distributed rather inhomogeneously.

The present study investigates whether 3He-MRI is capable of differentiating BOS from normal lung grafts, based on the measurements of the intrapulmonary pO_2 measured by oxygen-sensitive ^{3}He-MRI. This might help to better delineate the role of functional ^{3}He-MRI in the early detection of OB.

Materials and methods

Patients

Approval of the University's Ethics Committee and written informed patient consent were obtained for follow-up after lung transplantation including functional ^{3}He-MRI.

The cohort of this retrospective evaluation consisted of 12 patients (three female, nine male) aged between 39 and 61 years (median, 51). There were four double-lung recipients and eight single-lung recipients. The underlying disease necessitating lung transplantation was terminal emphysema in eight cases (including two cases with α-1-antitrypsin deficiency) and idiopathic pulmonary fibrosis in the remaining four (including two with acute interstitial pneumonia). Two of these patients contributed two datasets during follow-up, so a total of 14 datasets from these 12 patients were used for postprocessing. Of these datasets, eight were acquired in normal grafts, and six in presence of a clinical diagnosis of BOS. The cohort was selected from a group of 23 consecutively scanned lung transplant recipients during a period of 26 months.

Conventional follow-up and diagnosis of BOS were performed according to current recommendations of the International Society for Heart and Lung Transplantation, including serial pulmonary function testing (PFT) [17]. BOS was diagnosed on grounds of PFT deterioration if the ratio between current forced expiratory volume in 1 s (FEV1) and the best post-operative FEV1 became smaller than 0.81.

Inclusion criterion for this observational series was an oxygen-sensitive MRI dataset of diagnostic quality. Image series with low signal-to-noise ratio (SNR$\leq$3) due to low gas intake, very advanced states of BOS and prematurely aborted breath-holding were excluded from the study.

^{3}He-Gas

Polarization, storage, transport and application of ^{3}He have been described in detail elsewhere [18, 19]. We used ^{3}He polarized to 40–45% by metastability exchange optical pumping. The ^{3}He gas was administered to the patients using a computer-controlled application device. The device was connected to an intensive care-type ventilator (Servo

Table 1 Tabulated results of all evaluated datasets, including ventilation defect percentage ($SDpO_2$ standard deviation of oxygen partial pressure)

Dataset	BOS	pO_2 (mbar)	$SDpO_2$ (mbar)	Ventilation defect (%)
1	+	106	57	10
2	+	131	40	30
3	+	129	54	35
4	+	110	17	87.5
5	+	79	45	25
6	+	86	42	10
7	–	143	31	7.5
8	–	121	17	5
9	–	155	23	4
10	–	141	37	10
11	–	167	60	5
12	–	149	26	15
13	–	108	39	4
14	–	179	38	5

900 C, Siemens Medical Solutions, Erlangen, Germany) and operating in the pressure-support mode, in order to allow a comfortable spontaneous breathing pattern. For imaging approximately 300 ml of hyperpolarized ^{3}He were administered within a single breath to the patient.

Imaging

All measurements were performed on a 1.5-T clinical scanner (Magnetom Vision, Siemens Medical Solutions, Erlangen, Germany) tuned to the Larmor frequency of ^{3}He (48.5 MHz). The scanner was equipped with a broadband amplifier and a dedicated certified double resonant (^{1}H and ^{3}He) bird cage coil (Fraunhofer Institut, St. Ingbert, Germany) for transmission and reception of radio frequency pulses. We used a spoiled gradient echo pulse sequence oriented coronally with the following parameters: repetition time 11 ms, echo time 4.2 ms, flip angle <10°. Omission of a slice selection gradient lead to "single slice" projection images. In plane resolution was 3.95×2.5 mm at an acquisition matrix of 81×128 and a field of view of 320 mm. A double-acquisition technique allowed for mathematical separation of the effects of radio frequency pulses and T1 relaxation of ^{3}He due to the presence of molecular oxygen. This included two imaging series, consisting of eight images, with each series acquired during inspiratory breath hold. In both series, all parameters had to be kept constant (including inspired gas and ^{3}He volumes) except the inter-scan interval. This parameter was set to 1.005 s in the first, and 3, 4, or 5 s in the second imaging series, the latter depending on the patients' capability to hold their breath [15].

During the same imaging session, ^{3}He spin density images were acquired using the same scanner and coil. This was done during inspiratory breath-hold using a two-dimensional spoiled gradient echo pulse sequence. Images were oriented coronally and provided a slice thickness of 10–15 mm with

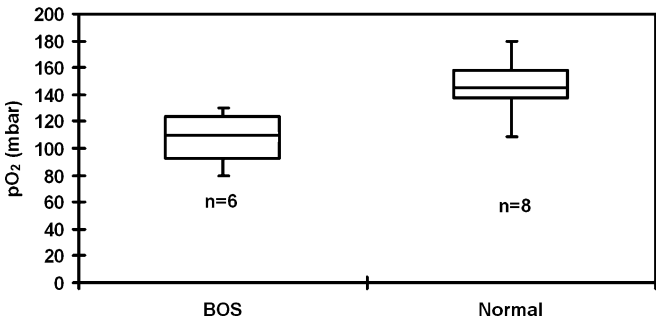

Fig. 1 Intrapulmonary pO_2 levels in BOS affected and normal lung grafts [plot depicting median, 25th and 75th percentiles (*box*), and minimum and maximum values (*whiskers*)]. There is a clear tendency for lower pO_2 values in the BOS group

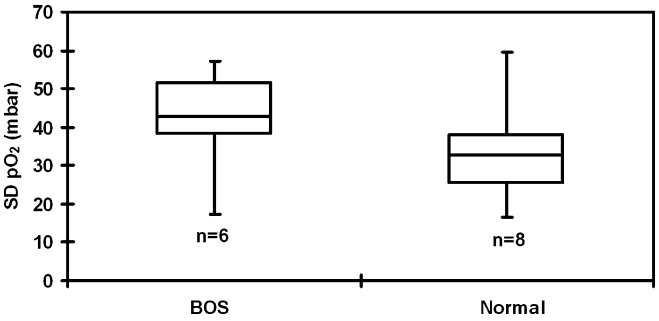

Fig. 2 Distribution of standard deviations of intrapulmonary pO_2 (box-whisker plot). Standard deviation is larger in patients suffering from BOS, reflecting a greater inhomogeneity of intra-pulmonary pO_2 distribution in this disease [plot depicting median, 25th and 75th percentiles (*box*), and minimum and maximum values (*whiskers*) of intra-individual pO_2 standard deviations]

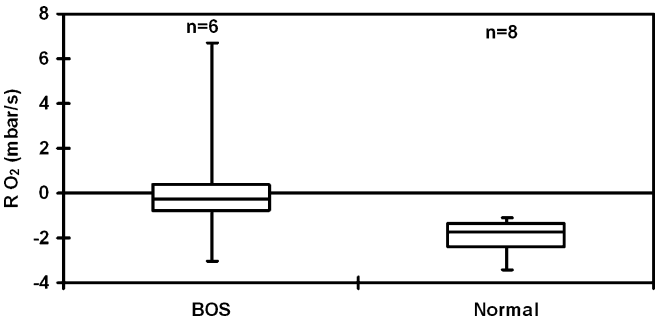

Fig. 3 Decrease rate (RO_2) of intrapulmonary pO_2 during breath-hold (box-whisker plot). A smaller RO_2 is an indirect indicator that oxygen uptake is lower in BOS when compared with normal lung grafts [plot depicting median, 25th and 75th percentiles (*box*), and minimum and maximum values (*whiskers*)]

Table 2 Tabulated results for the assumption of a non-Gaussian (median, inter-quartile range, range) and a Gaussian (mean, standard deviation, confidence interval) distribution (*IQR* interquartile range, *SD* standard deviation, *CI* confidence interval at $\alpha=0.050$)

		BOS	Normal
pO_2 (mbar)	Median	108	146
	IQR	33	21
	Range	52	71
	Mean	107	146
	SD	34	13
	CI	27	9
$SDpO_2$ (mbar)	Median	43	34
	IQR	13	13
	Range	40	43
	Mean	42	34
	SD	13	13
	CI	10	9
RO_2 (mbar)	Median	−0.38	−1.75
	IQR	1.24	1.08
	Range	9.69	2.34
	Mean	0.24	−1.99
	SD	3.05	0.83
	CI	2.4	0.55
Ventilation defect (%)	Median	28	5
	IQR	20	3
	Range	78	11
	Mean	33	7
	SD	29	4
	CI	23	3

an interslice gap of 2–5 mm (repetition time 11 ms, echo time 4.2 ms, flip angle 10°, centric reordering, in-plane resolution 4.2×2.7 mm, matrix 81×128, field of view 340 mm, sinc interpolation to a 256 matrix).

Image evaluation

Images were transferred to a commercially available IBM-compatible PC. An in-house developed software based on PV-Wave (Visual Numerics, Boulder, Colo.) was used for post-processing [20, 21]. The software is able to read image files in the DICOM standard and automatically excludes regions with a SNR of 3.0 or less. Filtering in the image domain reduced remaining noise. The software calculates the intrapulmonary pO_2 following the physical relationship between noise-corrected signal intensity (A) decay in two series of n images each, taken at different interscan delays τ_1 and τ_2, and pO_2:

$$1n(A_n, \tau_1/A_0) - 1n(A_n, \tau_2/A_0) = f(pO_2).$$

Results are displayed in colour-coded maps. In order to account for remaining image noise, a 2×2 matrix of image pixels was averaged giving the final 64×64 matrix, to be analysed for pO_2. The resultant in-plane resolution was 5×5 mm. The software calculates mean pO_2 and its standard deviation as well as the pO_2 decrease rate during the period of apnea while the imaging process takes place (RO_2). In case of unilateral lung transplants only the grafts underwent evaluation.

Spin density images were assessed for ventilation defects by two observers with several years practice in interpreting ^{3}He-images. They were blinded to patient history except for transplant status (single, right, left, double). The total volume of ventilation defects was estimated as percentage of total lung volume and expressed as means of both observers' results.

Statistical analysis

Data analysis was limited to descriptive statistics and graphic displays using box-whisker plots; significance testing, as well as the calculation of an interobserver agreement in the assessment of ventilation defects, was omitted due to the small study sample. Descriptive comparisons were made of mean intrapulmonary pO_2, intraindividual pO_2 standard deviation in order to describe

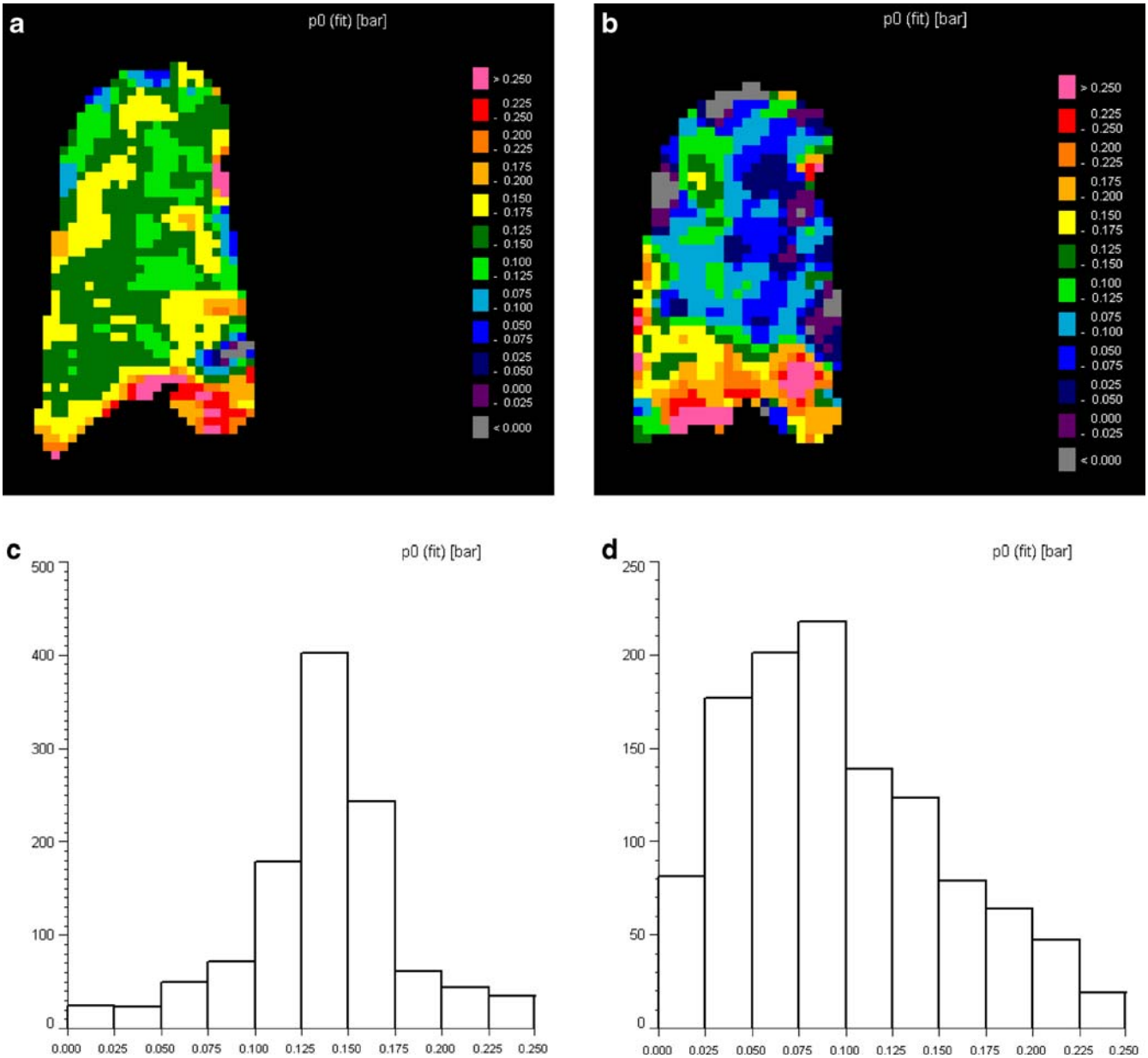

Fig. 4 **a** Intrapulmonary pO_2-map of a patient with a normal lung graft of a 42-year-old female after right-sided lung transplantation for terminal emphysema. **b** A pO_2 map of the same patient after development of BOS, with a decline of FEV_1 of 30% of her best post-operative FEV_1. **c** pO_2 histogram of the same patient at normal graft function, and **d** after development of BOS. The diminished and more inhomogeneous intrapulmonary pO_2 after BOS development can be well appreciated in the colour-coded maps as well as in the respective pO_2 histograms

homogeneity of its distribution and for mean decrease rate of pO_2 during apnea.

A systematic error towards lower pO_2 in image sets with poor SNR, which could be due to the influence of noise on the post-processing results, was studied by regression analysis of SNR and pO_2 data.

Results

Median intrapulmonary pO_2 in grafts of patients with diagnosed BOS was 108 mbar (range, min 79 mbar, max 131 mbar, see also Table 1), compared with an intrapulmonary pO_2 of 146 mbar (median; range, min 108 mbar,

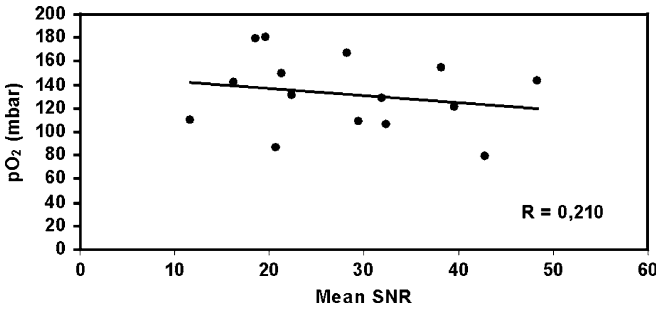

Fig. 5 Correlation between intrapulmonary pO_2 and SNR for all datasets. The low correlation coefficient reflects that lower pO_2 measurements in BOS grafts compared with normal lung grafts are very probably not due to a systematical error in pO_2 calculation routines related to poor SNR

max 179 mbar) in normal grafts. There was an overall trend towards lower intrapulmonary pO_2 levels in BOS patients shown by Fig. 1. In BOS patients, intrapulmonary pO_2 had a wider distribution, indicating a greater degree of ventilation-perfusion inhomogeneity (Fig. 2). Median standard deviation was 43 mbar in BOS patients versus 34 mbar in those with normal lung grafts. RO_2, i.e. pO_2 decrease rate during breath-holding, was less steep in BOS patients (median, −0.38 mbar/s breath-hold) than in unaffected patients (median, −1.75 mbar/s breathhold) (Fig. 3). As the number of study participants is low, Table 2 lists results for assumptions of Gaussian and non-Gaussian distribution.

Colour-coded maps showed a normal mean intrapulmonary pO_2 level with a quite homogeneous distribution in normal lung grafts, but lower and inhomogeneously distributed pO_2 levels in patients suffering from BOS (Fig. 4). Accordingly, ventilation defects were smaller in normal grafts. Patients with normal grafts presented with a median ventilation deficit of 5% (min 4%, max 15%) versus BOS patients with 28% (min 10%, max 88%).

Regression analysis did not detect any systematic linear relationship between SNR data and pO_2 measurements (r=0.21, Fig. 5). A systematic error towards lower pO_2 in lung images displaying poor SNR, like those affected by BOS, was therefore not substantiated.

Discussion

In 12 recipients of unilateral or bilateral lung transplants, oxygen-sensitive ^{3}He-MRI was added to post-transplant follow-up studies. In a total of 14 datasets, those from patients with normal lung grafts were compared with those from patients diagnosed with BOS. Analysis of intrapulmonary pO_2 data of the grafts demonstrated overall lower and more inhomogeneously distributed intrapulmonary pO_2 in patients diagnosed with BOS when compared with patients with an unaffected graft.

As a first step toward the goal of earlier non-invasive diagnosis of BOS, the technique and findings of this study confirm the predicted reduction of mean intrapulmonary pO_2 and greater inhomogeneity of its distribution in clinically manifest BOS. The study showed that the pO_2 decrease rate during apnea (RO_2) was smaller in BOS grafts than in clinically unaffected transplants. Patients not affected by BOS showed results similar to those determined in healthy volunteer subjects (mean±SD, 153±11 mbar) reflecting a normal ventilation and oxygen exchange [22].

A major limitation of the technique is demonstrated in the pO_2 maps of Fig. 4. One of the intrinsic disadvantages is that oxygen sensitive ^{3}He-MRI is critically dependent on alveolar entry of sufficient amounts of hyperpolarized ^{3}He gas. When a lung area contains no signal due to hypoventilation, no pO_2 can be determined. However, such areas are easily delineated in spin density MR images of the lung as ventilation defects. It has been demonstrated in previous studies that patients affected by BOS show more and larger ventilation defects than non-affected patients [7, 23].

There is a variety of other conditions that may cause reduction and inhomogeneity of intrapulmonary pO_2 distribution. Such abnormalities are known to occur in acute pulmonary embolism [24–27], in chronic thromboembolic pulmonary hypertension, as well as in pulmonary fibrosis or emphysema [1, 28, 29].

A pO_2 analysis based on images with low SNR may theoretically introduce a systematical measurement error because of the magnitude reconstruction of the MR images [30]. To study the relevance of this bias, image SNR and resultant pO_2 were correlated. We found a nonsignificant correlation with a coefficient r=0.21, which does not definitively exclude SNR dependency of the pO_2 measurements, but indicates at least minor importance.

There are several limitations to the present study. First, the small and relatively inhomogeneous study sample, with incomplete independence of compared groups, allows only a rather conservative interpretation of the results, and calls for further confirmation in larger cohorts. Technically, the pulse sequence applied for pO_2 measurement is a two-dimensional sequence without slice selectivity. Such projection images are robust against diffusion of ^{3}He polarization out of, or into, an imaged slice during the measurement interval, but they are inherently of restricted spatial resolution. First steps have been taken to develop and validate three-dimensional imagimg sequences, which provide marked spatial resolution and are, at the same time, robust against molecular diffusion effects [31, 32]. Finally, SNR remains a pivotal issue in oxygen-sensitive ^{3}He MRI. The gas used in the present study was polarized to a grade of 40–45%. Meanwhile, new gas polarizers have been developed which achieve polarization grades of up to 60%. Higher polarization is expected to improve accuracy of ^{3}He-MRI based pO_2 measurements as the error produced by image noise is decreased.

Currently, a non-invasive, sensitive and specific method to detect BO in lung transplant recipients is lacking [8–10]. Nevertheless, early detection of the disease is crucial for timely adaptation of the immunosuppressant regimen, in order to preserve as much graft function as possible [33–35]. Although ^{3}He-MRI may not prove to offer sufficient sensitivity and specificity to serve as a single diagnostic tool for BO detection, it may become of diagnostic use when combined with other imaging methods [36], e.g. to exclude infectious causes for deterioration of respiratory function [37]. Also, the regional information derived from ^{3}He-MRI may provide a road map for transbronchial biopsies, in order to target the most severely affected areas at the least possible discomfort for the patient.

Conclusion

Oxygen sensitive ^{3}He-MRI appears capable to differentiate pO_2 level grades, distribution and uptake between normal lung grafts and those affected by BOS in lung transplant recipients. Intrapulmonary pO_2 determined by oxygen sensitive ^{3}He-MRI, and its spatial and temporal distribution analysis might become a valuable supplement to current methods for the assessment and follow-up of lung transplant recipients.

Acknowledgements The study was supported by the German Research Society (DFG, FOR 474) as well as in part by the research grant "Physiological 3He Imaging of the Lung" Nycomed Amersham plc, UK.

References

1. Eberle B, Markstaller K, Lill J, Deninger A, Schreiber W, Mayer E, Kauczor H-U, Weiler N (2000) Oxygen-sensitive 3He magnetic resonance imaging of the lungs in patients after unilateral lung transplantation. Am J Resp Crit Care Med 161:A718
2. Kauczor H-U, Hanke A, Van Beek EJ (2002) Assessment of lung ventilation by MR imaging: current status and future perspectives. Eur Radiol 12:1962–1970
3. Ley S, Zaporozhan J, Morbach A, Eberle B, Gast KK, Heussel C-P, Biedermann A, Mayer E, Schmiedeskamp J, Stepniak A, Schreiber WG, Kauczor H-U (2004) Functional evaluation of emphysema using diffusion-weighted 3helium-magnetic resonance imaging, high-resolution computed tomography, and lung function tests. Invest Radiol 39(7):427–434
4. Schreiber WG, Weiler N, Kauczor HU, Markstaller K, Eberle B, Hast J, Surkau R, Grossmann T, Deninger A, Hanisch G, Otten EW, Thelen M (2000) Ultraschnelle MRT der Lungenventilation mittels hochpolarisiertem Helium-3 [Ultrafast MRI of lung ventilation using hyperpolarized helium-3]. Fortschr Roentgenstr 172(2):129–133
5. Gast KK, Puderbach M, Rodriguez I, Eberle B, Markstaller K, Knitz F, Schmiedeskamp J, Weiler N, Schreiber W, Mayer E, Thelen M, Kauczor H (2003) Distribution of Ventilation in Lung transplant recipients: evaluation by Dynamic ^{3}He-MRI with lung motion correction. Invest Radiol 38:341–348
6. Gast KK, Viallon M, Eberle B, Lill J, Puderbach M, Hanke A, Schmiedeskamp J, Kauczor H-U (2002) MR Imaging in lung transplant recipients using hyperpolarized 3He: comparison with CT. J Magn Reson Imag 15:268–274
7. Gast KK, Zaporozhan J, Ley S, Biedermann A, Knitz F, Eberle B, Schmiedeskamp J, Heussel CP, Mayer E, Schreiber WG, Thelen M, Kauczor HU (2004) ^{3}He-MRI in follow-up of lung transplant recipients. Eur Radiol 14:78–85
8. Ruppel GL (1997) Spirometry. Respir Care Clin N Am 3:155–181
9. Kramer MR, Stoehr C, Whang JL, Berry GJ, Sibley R, Marshall SE, Patterson GM, Starnes VA, Theodore J (1993) The diagnosis of obliterative bronchiolitis after heart-lung and lung transplantation: low yield of transbronchial lung biopsy. J Heart Lung Transplant 12(4):675–681
10. Lee ES, Gotway MB, Reddy GP, Golden JA, Keith FM, Webb WR (2000) Early bronchiolitis obliterans following lung transplantation: accuracy of expiratory thin-section CT for diagnosis. Radiology 216:472–477
11. Altes T, Powers P, Knight-Scott J, Rakes G, Platts-Mills T, de Lange E, Alford B, Mugler JI, Brookeman J (2001) Hyperpolarized 3He MR Lung Ventilation Imaging in Asthmatics: Preliminary Findings. J Magn Reson Imag 13:378–384
12. van Beek E, Hill C, Woodhouse N, Fichele S, Fleming S, Howe B, Bott S, Wild J, Taylor C (2007) Assessment of lung disease in children with cystic fibrosis using hyperpolarized 3-Helium MRI: comparison with Shwachman score, Chrispin-Norman score and spirometry. Eur Radiol 17:1018–1024
13. Salerno M, de Lange E, Altes T, Truwit J, Brookeman J, Mugler J (2002) Emphysema: hyperpolarized Helium3 diffusion MR imaging of the lungs compared with spirometric indexes—initial experience. Radiology 222:252–260
14. van Beek EJ, Wild JM, Kauczor HU, Schreiber W, Mugler JPr, de Lange EE (2004) Functional MRI of the lung using hyperpolarized 3-helium gas. J Magn Reson Imaging 20(4):540–554
15. Eberle B, Weiler N, Markstaller K, Kauczor H, Deninger A, Ebert M, Grossmann T, Heil W, Lauer LO, Roberts TP, Schreiber WG, Surkau R, Dick WF, Otten EW, Thelen M (1999) Analysis of intrapulmonary O(2) concentration by MR imaging of inhaled hyperpolarized helium-3. J Appl Physiol 87(6):2043–2052
16. Fischer MC, Kadlecek S, Yu J, Ishii M, Emami K, Vahdat V, Lipson DA, Rizi RR (2005) Measurements of regional alveolar oxygen pressure using hyperpolarized 3He MRI. Acad Radiol 12 (11):1430–1439
17. Cooper JD, Billingham M, Egan T, Hertz M, Higenbottam T, Lynch J, Mauer J, Paradis I, Patterson GA et al (1993) A working formulation for the standardization of nomenclature and for clinical staging of chronic dysfunction in lung allografts: International Society for Heart and Lung Transplantation. J Heart Lung Transplant 12:713–716

18. Gast KK, Ley S, Zaporozhan J, Puderbach M, Eberle B, Biedermann A, Knitz F, Schmiedeskamp J, Weiler N, Schreiber W, Mayer E, Heussel C, Thelen M, Kauczor H (2003) Reformatierungen als Lösungsansatz für die Problematik der unterschiedlichen Schichtführung beim Vergleich von ^{3}He-MRT und HR-CT der Lunge [Reformation as proposed solution for the problem of sectioning different levels with 3He-MRT and HR-CT of the chest]. Fortschr Röntgenstr 175:786–790
19. Wild JM, Schmiedeskamp J, Paley MN, Filbir F, Fichele S, Kasuboski L, Knitz F, Woodhouse N, Swift A, Heil W, Mill GH, Wolf M, Griffiths PD, Otten E, van Beek EJ (2002) MR imaging of the lungs with hyperpolarized helium-3 gas transported by air. Phys Med Biol 47:185–190
20. Lehmann F, Eberle B, Markstaller K, Gast KK, Schmiedeskamp J, Blümler P, Kauczor HU, Schreiber WG (2004) Ein Auswerteprogramm zur quantitativen Analyse von Messungen des alveolären Sauerstoffpartialdrucks (pAO2) mit der sauerstoffsensitiven 3He-MR-Tomographie [A software program for quantitative analysis of alveolar oxygen partial pressure (pAO2) with oxygen-sensitive 3He-MRI]. Fortschr Röntgenstr 176 (10):1390–1398
21. Schreiber WG, Morbach AE, Stavngaard T, Gast KK, Herweling A, Sogaard LV, Windirsch M, Schmiedeskamp J, Heussel C, Kauczor H (2005) Assessment of lung microstructure with magnetic resonance imaging of hyperpolarized Helium-3. Respir Physiol Neurobiol 148(1–2): 23–42
22. Deninger AJ, Eberle B, Ebert M, Grossmann T, Hanisch G, Heil W, Kauczor HU, Markstaller K, Otten E, Schreiber W, Surkau R, Weiler N (2000) (3)he-MRI-based measurements of intrapulmonary p(O2) and its time course during apnea in healthy volunteers: first results, reproducibility, and technical limitations. NMR Biomed 13 (4):194–201
23. McAdams HP, Palmer SM, Donnelly LF, Charles HC, Tapson VF, MacFall JR (1999) Hyperpolarized 3He-enhanced MR imaging of lung transplant recipients: preliminary results. Am J Roentgenol 173:955–959
24. Fischer MC, Kadlecek S, Yu J, Ishii M, Emami K, Vahdat V, Lipson DA, Rizi RR (2005) Measurements of regional alveolar oxygen pressure using hyperpolarized 3He MRI. Acad Radiol 12 (11):1430–1439
25. Rizi RR, Baumgardner J, Ishii M, Spector ZZ, Edvinsson J, Jalali A, Yu J, Itkin M, Lipson DA, Gefter W (2004) Determination of regional VA/Q by hyperpolarized 3He MRI. Magn Reson Med 52(1):65–72
26. Eberle B, Markstaller K, Stepniak A, Viallon M, Kauczor H-U (2002) 3Helium-MRI-Based Assessment of regional gas exchange impairment during experimental pulmonary artery occlusion. Anesthesiology 96:A1309
27. Kadlecek S, Rizi RR (2005) New diagnostic tests for pulmonary emboli. Acad Radiol 12(2):133–135
28. Hopkins S, Levin D, Emami K, Kadlecek S, Yu J, Ishii M, Rizi RR (2007) Advances in magnetic resonance imaging of lung physiology. J Appl Physiol 102(3):1244–1254
29. Markstaller K, Gast K, Herweling A, Schmiedeskamp J, Mayer E, Kauczor H, Eberle B (2003) Detektion regionaler Gasaustauschstörungen bei chronischer thrombembolischer pulmonaler Hypertonie (CTEPH) mittels 3Helium-MRT. Abstractband Deutscher Anästhesiecongress: 194
30. Henkelman RM (1985) Measurement of signal intensities in the presence of noise in MR images. Med Phys 12 (2):232–233
31. Gast KK, Schreiber WG, Herweling A, Lehmann F, Erdös G, Schmiedeskamp J, Kauczor H-U, Eberle B (2005) Two-dimensional and three-dimensional oxygen mapping by ^{3}He-MRI - validation in a lung phantom. Eur Radiol 15(9):1915–1922
32. Wild J, Fichele S, Woodhouse N, Paley M, Kasuboski L, van Beek E (2005) 3D volume-localized pO2 measurement in the human lung with 3He MRI. Magn Reson Med 53:1055–1064
33. Estenne M, Hertz MI (2002) Bronchiolitis obliterans after human lung transplantation. Review. Am J Respir Crit Care Med 166:440–444
34. Frost AE, Keller CA, Noon GP, Short HD, Cagle PT (1995) Outcome of the native lung after single lung transplant. Multiorgan Transplant Group. Chest 107(4):981–984
35. Izbicki G, Shitrit D, Aravot D, Sulkes J, Saute M, Sahar G, Kramer M (2002) Improved survival after lung transplantation in patients treated with tacrolimus/mycophenolate mofetil as compared with cyclosporine/azathioprine. Transplant Proc 34:3258–3259
36. Zaporozhan J, Ley S, Gast KK, Schmiedeskamp J, Biedermann A, Eberle B, Kauczor HU (2004) Functional analysis in single-lung transplant recipients: a comparative study of high-resolution CT, 3He-MRI, and pulmonary function tests. Chest 125(1):173–181
37. Collins J, Muller NL, Kazerooni EA, Paciocco G (2000) CT findings of pneumonia after lung transplantation. AJR Am J Roentgenol 175:811–818